Thesis for the Degree of Master of Engineering

A Simplified Model of Interlocked Caisson System for Damage Assessment

by

Huynh Thanh Canh

Department of Ocean Engineering

The Graduate School

Pukyong National University

August 2013

A Simplified Model of Interlocked Caisson System for Damage Assessment

인터록킹된 케이슨 시스템의 손상평가를 위한 단순화 모델

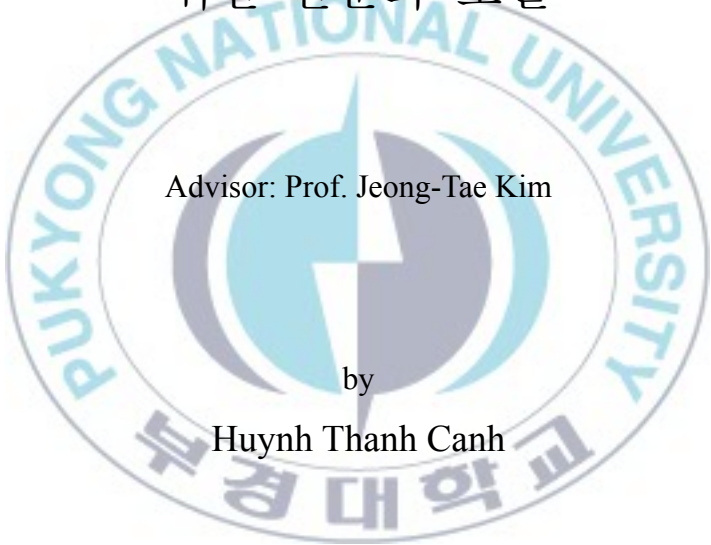

Advisor: Prof. Jeong-Tae Kim

by

Huynh Thanh Canh

A thesis submitted in partial fulfillment of the requirements
for the degree of
Master of Engineering

in Department of Ocean Engineering, the Graduate School,
Pukyong National University

August 2013

Huynh Thanh Canh의 공학석사 학위논문을 인준함

2013년 8월

주 심 공학박사 김 윤 태 (인)

위 원 공학박사 나 원 배 (인)

위 원 공학박사 김 정 태 (인)

TABLE OF CONTENTS

LIST OF FIGURES

LIST OF TABLES

A Simplified Model of Interlocked Caisson System for Damage Assessment

Huynh Thanh Canh

Department of Ocean Engineering
The Graduate School
Pukyong National University

ABSTRACT

The objective of this study is to present a simplified model of interlocked caisson system which can be used for dynamic analysis and damage assessment. The following approaches are performed to obtain the objective. Firstly, a conceptual dynamic model of the interlocked caisson system is designed on the basis of the characteristics of existing harbor caisson structures. A mass-spring-dashpot model considering only the sway motion is proposed. In the simplified model, each caisson unit is connected to adjacent ones by adding springs and dashpots to represent the condition of interlocking mechanisms. Secondly, the simplified model of the interlocked caisson system is evaluated for vibration analysis. A 3-D finite element model of the caisson system is utilized to examine the accuracy of the simplified model's vibration responses. Thirdly, the simplified model of the caisson system is employed for damage assessment. A damage detection method based on modal strain energy is formulated to localize damage in the caisson system.

CHAPTER 1
INTRODUCTION

1.1 Background

A breakwater is constructed to provide safe spaces for ship anchorage and to protect harbor facilities from the action of waves. It is designed to absorb the wave energy from open sea, either by its mass or by revetment slope with armor units. Among various breakwater types, caisson breakwaters have been widely used since they provide extremely stable structures even in rough and deep seas (Takahashi, 2002).

Over the last decades, severe failure events of caisson breakwaters have been reported from Japan, Italy, Spain, and etc. (Oumeraci, 1994). Despite considerable lessons that have been learned from those failure events (Franco, 1994; Oumeraci, 1994; Tanimoto and Takahashi, 1994), the structural failures have still been observed in recent years (Maddrell, 2005; Taro, 2012). Meanwhile, structural health monitoring (SHM) has become the key to ensure the safety and serviceability of caisson breakwater systems. The adequate assessment of the structural safety and performance is prerequisite to estimate the failure probabilities for the design and maintenance of the breakwater system (Oumeraci et al., 2001).

Related to damage types in caisson breakwaters, it can be clarified into sliding, overturning and settlement. They are called global damages. Before the actual collapse occurs, it is generally preceded by small defects, so-called local damages such as seabed scour or erosion at the foundation (Oumercaci, 1994). Therefore, it is very important to capture the incipient local defects in structure-foundation interface in time before they become the global damages.

Up to now, vibration-based damage monitoring for civil structures has been widely studied via examining the change in measured vibration response (Doebling et al., 1996; Sohn et al., 2003). The problems concerned with structural damage detection, localization and characterization can be

solved by damage detection theories such as modal sensitivity methods, modal flexibility methods, genetic algorithm, artificial neural network, etc. (Wu et al., 1992; Pandey and Biswas, 1994; Kim and Stubbs, 1995; Yun and Bahng 2000; Chou and Ghaboussi, 2001; Koo et al., 2009; Park et al., 2009). Also, many sensor systems have been proposed for vibration-based SHM of civil structures. However, most of SHM systems have been applied to inland structures such as bridges and buildings (Wong, 2004; Glisic et al., 2005; Jang et al., 2010; Ho et. al, 2012). Many challenges still remain to develop efficient SHM systems for offshore structures such as breakwaters.

Over the past three decades, many researchers have investigated global structural failures of caisson-type breakwaters such as overturning, sliding or settlement by numerical analyses as well as experimental model tests (Yamamoto et al., 1981; Kobayashi et al., 1987; Sekiguchi and Ohmaki, 1992; Sekiguchi and Kobayashi, 1994). A few researchers have analyzed vibration responses of coastal structures considering soil-structure or fluid-soil-structure interactions (Yang et al., 2001, Kim et al., 2005). Recently, a few researchers have attempted to monitor the health status of caisson structures using changes in modal parameters (Park et al., 2011; Lee et al., 2011 and 2012; Yoon et al., 2012). Those studies have mostly concentrated on mono-caisson systems which have potential damage in structure-foundation interface. For damage assessment in a real caisson breakwater, the following main issues should be considered: (1) the submerged condition of the coastal structure limits the accessibility for vibration measurement; and (2) the harbor caisson system consists of multiple caisson segments which are normally interconnected with each other by shear-keys to resist against the incident wave force acting perpendicular to the front wall.

On the demand to support dynamic analysis of caisson-type breakwater, a few simplified dynamic models were proposed with small differences in the recent years (Smirnov and Moroz, 1983; Marinski and Oumeraci, 1992; Goda, 1994; Oumeraci and Kortenhaus, 1994; Vink, 1997).

To simulate dynamic behaviors of a caisson, the analytical model of a rigid body on an elastic half-space foundation is usually used (Barkan, 1962; Richart, 1970). The elasticity of the foundation is described via the coefficient of soil reaction (so-called modulus of subgrade reaction or bed constant). However, most of the previous simplified models did not represent the effect of longitudinal caisson array. Therefore, a simplified model of interlocked caissons should be developed to improve the understanding of dynamic behaviors of the caisson system. Furthermore, the simplified model can be utilized to formulate a damage detection method for the health status assessment of the caisson systems.

Concerned with the above-mentioned issues, the simplified model of the interlocked caisson system is developed in this study.

1.2 Objective and Scope

This study presents a simplified model of interlocked caisson system which can be used for dynamic analysis and damage assessment. In order to achieve the goal, the following tasks are performed:

1. A conceptual dynamic model of the interlocked caisson system is designed on the basis of the characteristics of existing harbor caisson structures. The mass-spring-dashpot model allowing only the sway motion is proposed. In the simplified model, each caisson unit is connected to adjacent ones by adding springs and dashpots to represent the condition of interlocking mechanisms.
2. The simplified model of the interlocked caisson system is evaluated for vibration analysis. A 3-D finite element (FE) model of the caisson system is utilized to examine the accuracy of the simplified model's vibration responses.
3. The simplified model is employed for damage assessment. A damage detection method based on modal strain energy (MSE) is formulated to localize damage in the caisson system.

1.3 Organization of the Thesis

The remaining work is divided into 4 chapters. In Chapter 2, a conceptual dynamic model of interlocked caissons is designed based on the basis of the characteristics of existing harbor caisson structures. Structural parameters of the simplified model are identified. In Chapter 3, the simplified model of the interlocked caisson system is evaluated for vibration analysis. A caisson system of three units is selected as the target structure. Next, a 3-D FE model of the target caisson structure is established using SAP2000 software. Forced vibration analysis is performed to obtain vibration responses of the caisson system. Then, the 3-D FE model is simplified using the conceptual dynamic model proposed in Chapter 2. Vibration features (i.e., power spectral density, natural frequency and mode shape) of the simplified model are compared with those of the 3-D FE model for the validation of vibration analysis. In Chapter 4, the simplified model of the caisson system is employed for damage assessment. A damage detection method based on modal strain energy is formulated to localize damage the caisson system. Finally, Chapter 5 summarizes research details of this thesis and future researches on the simplified model of the interlocked caisson system for damage assessment.

CHAPTER 2
A SIMPLIFIED MODEL OF INTERLOCKED CAISSONS

2.1 Introduction

Simplified model of caisson-type breakwater is a model which is represented by a few degrees of freedom (DOFs) of the caisson such as translational and rotational motions. Over the last decades, many researchers have worked on developing simplified models of harbor caisson structures (Smirnov and Moroz, 1983; Marinski and Oumeraci, 1992; Goda, 1994; Oumeraci and Kortenhaus, 1994; Vink, 1997). To simulate dynamic behaviors of a caisson, the analytical model of a rigid body on an elastic half-space foundation is usually used (Barkan, 1962; Richart, 1970). The elasticity of the foundation is described via the coefficient of soil reaction (so-called modulus of subgrade reaction or bed constant). However, most of the previous simplified models did not represent the effect of longitudinal caisson array. In fact, each caisson unit in a caisson system interacts not only with surrounding media (i.e., sea water and soil) but also with adjacent units via their contacting interfaces (Lamberti and Marteinelli, 1998). Based on the existing caisson models, a mass-spring-dashpot array model is designed in this chapter.

2.2 Equations of Motion

As shown in Fig. 2.1, the caisson system is subjected to an impulsive breaking wave force that results in forced vibration responses. Since the wave action is usually perpendicular to the caisson array axis (i.e., x-direction), the vibration in the impact direction (i.e., y-direction) is relatively larger than other directions (Lee et al., 2011 and 2012; Yoon et al., 2012). Therefore, only the sway motion of caissons (i.e., y-direction) is taken into account in this study. Based on a few existing simplified models, a planar model of three interlocked caissons is proposed as shown in Fig. 2.2. In the simplified model, caissons are treated as rigid bodies on elastic half-space

foundations which can be described via the horizontal springs and dashpots. To represent the condition of interlocking mechanism, springs and dashpots are also simulated between adjacent caissons unit.

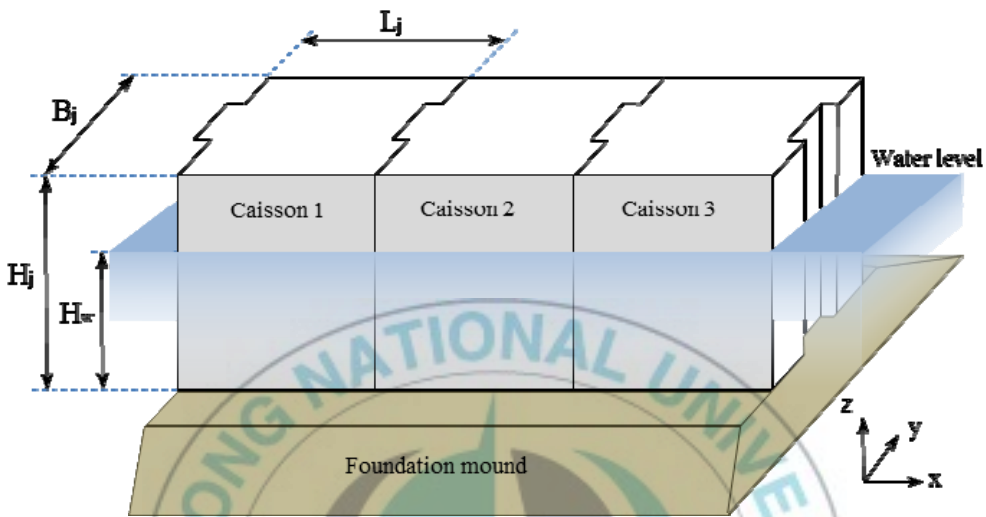

Fig. 2.1 A caisson system of three units

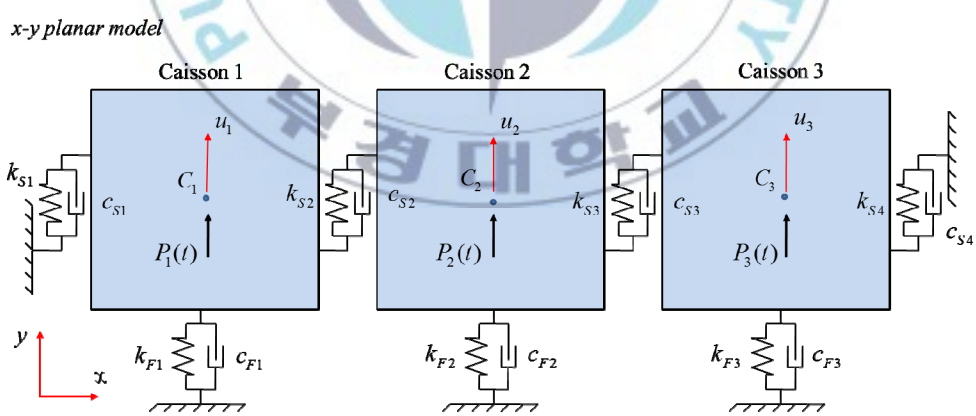

Fig. 2.2 Simplified dynamic model of three caisson units

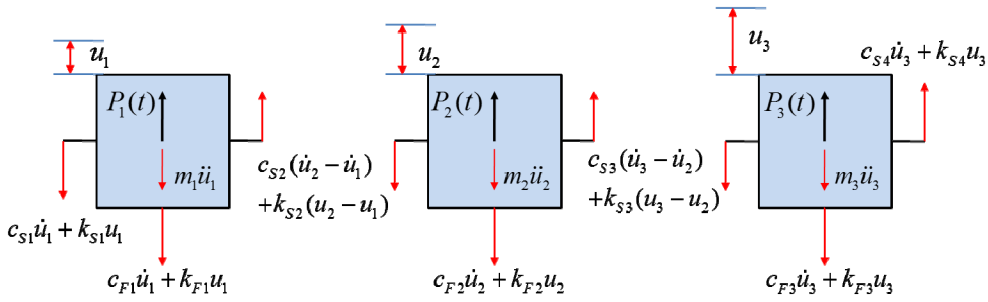

Fig. 2.3 Free-body diagrams of simplified dynamic model

The equations of motion obtained by equating to zero the sum of forces in the free body diagrams (see Fig. 2.3) as follows:

$$\begin{aligned}
&m_1\ddot{u}_1+(c_{F1}\dot{u}_1+k_{F1}u_1)+(c_{S1}\dot{u}_1+k_{S1}u_1)-\left[c_{S2}(\dot{u}_2-\dot{u}_1)+k_{S2}(u_2-u_1)\right]-P_1(t)=0\\
&m_2\ddot{u}_2+(c_{F2}\dot{u}_2+k_{F2}u_2)+\left[c_{S2}(\dot{u}_2-\dot{u}_1)+k_{S2}(u_2-u_1)\right]-\left[c_{S3}(\dot{u}_3-\dot{u}_2)+k_{S3}(u_3-u_2)\right]-P_2(t)=0\\
&m_3\ddot{u}_3+(c_{F3}\dot{u}_3+k_{F3}u_3)+\left[c_{S3}(\dot{u}_3-\dot{u}_2)+k_{S3}(u_3-u_2)\right]-(c_{S4}\dot{u}_3+k_{S4}u_3)-P_3(t)=0
\end{aligned} \quad (2.1)$$

where m_j is the total horizontal mass of the j^{th} caisson; k_{Fj} and c_{Fj} separately represent the y-directional spring and dashpot of the j^{th} caisson's foundation (j=1-3); k_{Sk} and c_{Sk} respectively represent the y-directional spring and dashpot of the k^{th} shear-key connection (k=1-4); $\ddot{u}_j, \dot{u}_j$ and u_j are, respectively, the horizontal acceleration, velocity and displacement of the j^{th} caisson; and $P_j(t)$ is the external force placed at the center of gravity of the j^{th} caisson.

The above differential equations can be written in a matrix notation as:

$$\begin{bmatrix} m_1 & 0 & 0 \\ 0 & m_2 & 0 \\ 0 & 0 & m_3 \end{bmatrix}\begin{Bmatrix} \ddot{u}_1 \\ \ddot{u}_2 \\ \ddot{u}_3 \end{Bmatrix}+\begin{bmatrix} c_{F1}+c_{S1}+c_{S2} & -c_{S2} & 0 \\ -c_{S2} & c_{F2}+c_{S2}+c_{S3} & -c_{S3} \\ 0 & -c_{S3} & c_{F3}+c_{S3}+c_{S4} \end{bmatrix}\begin{Bmatrix} \dot{u}_1 \\ \dot{u}_2 \\ \dot{u}_3 \end{Bmatrix}$$
$$+\begin{bmatrix} k_{F1}+k_{S1}+k_{S2} & -k_{S2} & 0 \\ -k_{S2} & k_{F2}+k_{S2}+k_{S3} & -k_{S3} \\ 0 & -k_{S3} & k_{F3}+k_{S3}+k_{S4} \end{bmatrix}\begin{Bmatrix} u_1 \\ u_2 \\ u_3 \end{Bmatrix}=\begin{Bmatrix} P_1(t) \\ P_2(t) \\ P_3(t) \end{Bmatrix} \quad (2.2a)$$

or $$[M]\{\ddot{u}\}+[C]\{\dot{u}\}+[K]\{u\}=\{P\} \quad (2.2b)$$

where [*M*], [*C*], and [*K*] are the mass, damping and stiffness matrices given, respectively, by:

$$[M]=\begin{bmatrix} m_1 & 0 & 0 \\ 0 & m_2 & 0 \\ 0 & 0 & m_3 \end{bmatrix} \tag{2.3}$$

$$[C]=\begin{bmatrix} c_{F1}+c_{S1}+c_{S2} & -c_{S2} & 0 \\ -c_{S2} & c_{F2}+c_{S2}+c_{S3} & -c_{S3} \\ 0 & -c_{S3} & c_{F3}+c_{S3}+c_{S4} \end{bmatrix} \tag{2.4}$$

$$[K]=\begin{bmatrix} k_{F1}+k_{S1}+k_{S2} & -k_{S2} & 0 \\ -k_{S2} & k_{F2}+k_{S2}+k_{S3} & -k_{S3} \\ 0 & -k_{S3} & k_{F3}+k_{S3}+k_{S4} \end{bmatrix} \tag{2.5}$$

and the terms $\{\ddot{u}\},\{\dot{u}\},\{u\}$ and $\{P\}$ are, respectively, the acceleration, velocity, displacement and external force vectors given by:

$$\{\ddot{u}\}=\begin{Bmatrix} \ddot{u}_1 \\ \ddot{u}_2 \\ \ddot{u}_3 \end{Bmatrix},\ \{\dot{u}\}=\begin{Bmatrix} \dot{u}_1 \\ \dot{u}_2 \\ \dot{u}_3 \end{Bmatrix},\ \{u\}=\begin{Bmatrix} u_1 \\ u_2 \\ u_3 \end{Bmatrix},\ \{P\}=\begin{Bmatrix} P_1(t) \\ P_2(t) \\ P_3(t) \end{Bmatrix} \tag{2.6}$$

2.3 Determination of Structural Parameters

Mass Parameter

When the caisson is oscillated by an impact load, the surrounding media (i.e., soil and water) are forced to move with the structure. Therefore, the total horizontal mass of the j^{th} caisson (m_j) includes not only the mass of the caisson itself ($m^{cai}{}_j$) but also the horizontal hydrodynamic ($m^{hyd}{}_j$) and the horizontal geodynamic masses ($m^{geo}{}_j$) as follows:

$$m_j = m_j^{cai} + m_j^{hyd} + m_j^{geo} \tag{2.7}$$

For calculating the horizontal hydrodynamic mass, the following equation presented by Oumeraci and Kortenhaus (1994) is used:

$$m_j^{hyd} = 0.543 L_j \rho_w H_w^{\,2} \tag{2.8}$$

in which the quantities L_j and H_w represent the j^{th} caisson's length and the water level, as shown in Fig. 2.1; and the quantity ρ_w is the mass density of sea water.

According to Richart et al. (1970), the horizontal geodynamic mass can be computed as:

$$m_j^{geo} = \frac{0.76\rho_s \left(\frac{B_j L_j}{\pi}\right)^{\frac{3}{2}}}{2-\nu} \tag{2.9}$$

where ρ_s and ν are respectively the mass density and Poisson's ratio of the foundation soil; and B_j is the j^{th} caisson's width, as sketched in Fig. 2.1.

Stiffness Parameter

It is commonly accepted in geotechnical engineering that the horizontal spring constant (k_{Fj}) of the elastic foundation is the function of the horizontal modulus of subgrade reaction *(b)* as, the j^{th} caisson width (B_j) and length (L_j), follows:

$$k_{Fj} = bL_jB_j \tag{2.10}$$

The modulus of subgrade reaction of various soil types, which has the unit of pressure per length, can be found in literature by Bowles (1996). The same formulas have also been adopted by Goda (1994) and Vink (1997).

Unlike the foundation mound, the theoretical basis for determination of the shear-keys' stiffness is weaker since it depends on the linking capacity between contacted units in the real caisson breakwater (Lamberti and Martinelli, 1998; Oumeraci et al., 2001). Normally, caisson segments are designed with the uniform linking capacity, where $k_{S2} = k_{S3}$. Since the rest

of caisson array is not represented in the planar model, the stiffness of the last shear-keys (i.e., k_{S1} and k_{S4}) is smaller than that of the middle shear-keys (i.e., k_{S2} and k_{S3}). This condition can be expressed as:

$$k_{S1} = k_{S4} = ak_{S2} = ak_{S3} \tag{2.11}$$

where a is an empirical value ranging from 0 to 1 (Lamberti and Martinelli, 1998). In computation, the stiffness parameters are obtained by adjusting the vibration responses of the simplified model to fit those of the 3-D FE model.

Damping Parameter

In this study, the Rayleigh damping, which is often used in the dynamic mathematical model, for simulation of dynamic hehaviors of structures is used to simulate the energy dissipation in the caisson system. The Rayleigh damping is assumed to be proportional to the mass and stiffness matrices (Wilson, 2004):

$$[C] = \alpha[M] + \beta[K] \tag{2.12}$$

in which α is the mass-proportional damping coefficient; and β is the stiffness-proportional damping coefficient. Due to the orthogonality conditions of the mass and stiffness matrices, this equation can be rewritten as:

$$\xi_n = \frac{1}{2\omega_n}\alpha + \frac{\omega_n}{2}\beta \tag{2.13}$$

where ξ_n is the critical-damping ratio for mode n; and ω_n is the n^{th} natural frequency.

If the damping ratios (e.g., ξ_i and ξ_j) corresponding to two specific frequencies (e.g., ω_i and ω_j) are known, the two Rayleigh damping factors (i.e., α and β) can be evaluated from the following equation:

$$\begin{bmatrix} \xi_i \\ \xi_j \end{bmatrix} = \frac{1}{2} \begin{bmatrix} \frac{1}{\omega_i} & \omega_i \\ \frac{1}{\omega_j} & \omega_j \end{bmatrix} \begin{bmatrix} \alpha \\ \beta \end{bmatrix} \tag{2.14}$$

When damping for both frequencies is set to an equal value, $\xi_i = \xi_j = \xi$, the Rayleigh damping factors are calculated as (Wilson, 2004):

$$\beta = \frac{2\xi}{\omega_i + \omega_j} \quad \text{and} \quad \alpha = \omega_i \omega_j \beta \tag{2.15}$$

CHAPTER 3
VALIDATION OF SIMPLIFIED MODEL FOR VIBRATION ANALYSIS

3.1 Introduction

The simplified model of the interlocked caisson system is evaluated for the accuracy of vibration analysis. Firstly, a caisson system consisting of three interlocked caisson units is selected as the target structure. Secondly, a 3-D FE model of the target structure is established using SAP2000 software. Forced vibration analysis is performed to examine dynamic behaviors of the target structure. Thirdly, the 3-D FE model is simplified using the proposed conceptual dynamic model presented in Chapter 2. Finally, vibration features such as power spectral density, natural frequency and mode shape of the simplified model are compared with those of the 3-D FE model.

3.2 Target Caisson Structure

A lab-scaled caisson system consisting of three concrete caisson modules (i.e., Caisson 1, Caisson 2 and Caisson 3) was chosen as the target caisson structure. The geometry of the target caisson-type breakwater is sketched in Fig. 3.1. As shown in the figure, caissons are designed with shear-key connections to prevent them from shear motions. The caissons are filled with sand and covered by concrete caps with the thickness of 0.06 m. The width, height and length of a caisson unit are 0.34 m, 0.4 m and 0.34 m, respectively. The foundation consists of a 0.08 m thick mound of medium-dense sand and a 0.02 m thick layer of medium gravel. The whole caisson system is placed on the sea bed of dense sand. The water depth measured from the sea bed at both sides of the caisson system is 0.42 m.

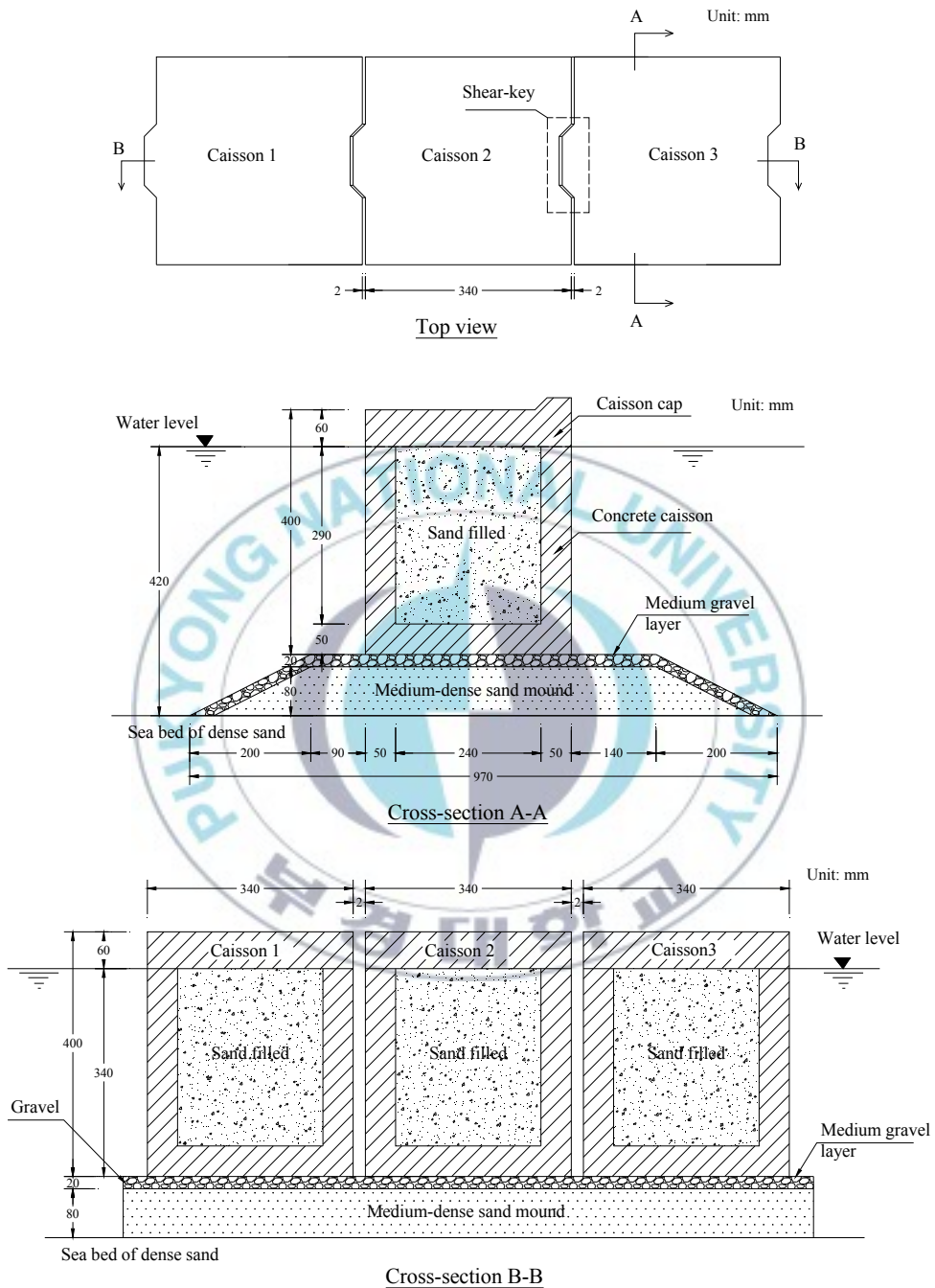

Fig. 3.1 Geometry of target caisson structure

The concrete properties and mix design are shown in Table 3.1. The elastic modulus of concrete is calculated using its 28-day compressive strength (i.e., 28 MPa) according to ACI Committee 318 (2005). The material properties of foundation soils (i.e., medium-dense sand and medium gravel) are selected using Handbook of Geotechnical Investigation and Design Tables (Look, 2007). The selected values are provided in Table 3.2.

Table 3.1 Concrete properties and mix design

Unit weight (kg/m^3)					28-day strength (MPa)
Water	Cement	Sand	Gravel	Admixture	
160	340	922	979	3.4	21
Mass density (kg/m^3)		Elastic modulus (GPa)		Poisson's ratio	
2400		24		0.2	

Table 3.2 Material properties of foundation soils

	Medium gravel	Medium-dense sand
Mass density (kg/m^3)	2100	2000
Elastic modulus (MPa)	50	30
Poisson's ratio	0.3	0.325

3.3 3-D FE Analysis of Target Caisson Structure

3.3.1 3-D FE Model

A 3-D FE model of the target caisson structure is simulated using SAP2000 software as shown in Fig. 3.2a. In the 3-D FE model, the elastic characteristic of the sea bed (dense sand) is described by an area spring system (see Fig. 3.2c). According to the previous experimental studies on foundation analysis by Bowles (1996), the spring constant for dense sand is recommended to be 64 to 128 MN/m/m^2. Therefore, 96 MN/m/m^2 is selected for the spring constant of the sea bed. The interlocking condition is simulated by y-directional 1-D links at the shear-keys, as described in Fig. 3.2b. In this study, the stiffness of links is assumed to be 25 MN/m/m^2. Due to additional hydrodynamic damping effects, the damping ratios of caisson breakwaters are relatively higher than those of general concrete structures (e.g., 3%). In the previous experimental studies by Gao et al. (1988), the damping ratios of real caisson structures are found to be 3.2-7.5%. Hence, 5% of the damping ratio is assumed for all modes in the 3-D FE model.

To simulate the submerged condition of the target caisson structure, the effective mass of sea water (M_w) is added to the 3-D numerical model, as shown in Fig. 3.2c. The added mass of sea water is calculated by Westergaard's hydrodynamic water pressure equation (Westergaard, 1933) as follows:

$$M_w = \int_{h_1}^{h_2} \frac{7}{8} \rho_w \sqrt{H_w h} \; .dh \tag{3.1}$$

where M_w is the hydrodynamic mass; ρ_w is the water density; H_w and h are the depth from water level to the foundation and that to the action point of hydrodynamic pressure, respectively. It should be noted that Eq. (2.8) is a simplified form of Eq. (3.1) when $h_1 = 0$ and $h_2 = H_w$.

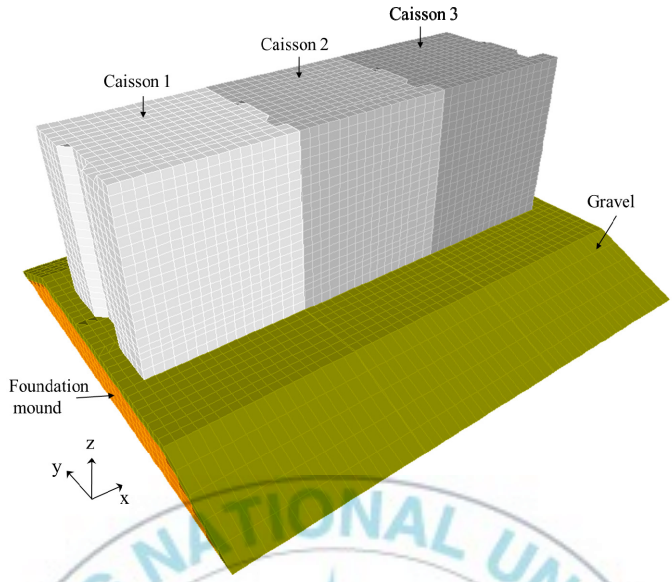

(a) 3-D FE model

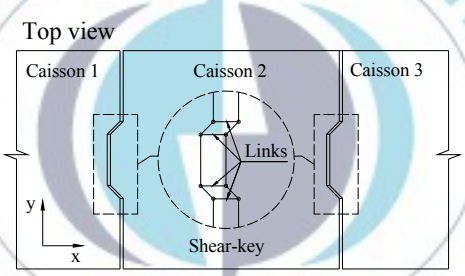

(b) Interlocking conditions

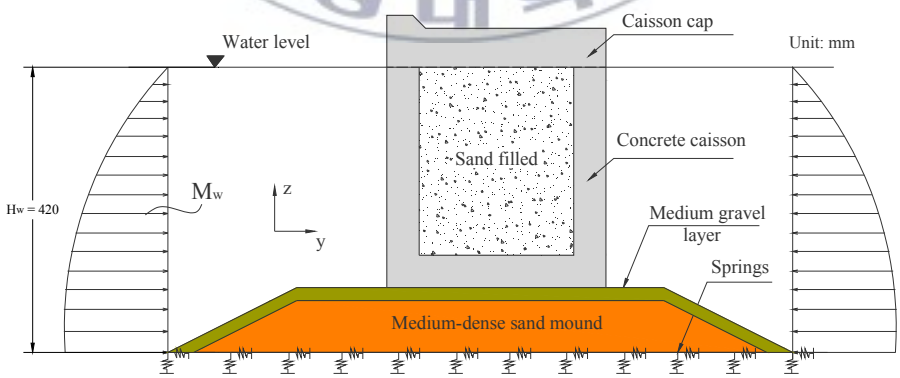

(c) Boundary conditions

Fig. 3.2 3-D FE model of target caisson structure

3.3.2 Forced Vibration Analysis

In order to obtain vibration responses of the caisson system, forced vibration analysis is designed considering limited accessibilities. An impact force, which has corresponding direction of incident wave (i.e., y-direction), is applied perpendicularly to the front wall of Caisson 2 as denoted in Fig. 3.3. The impact force is assumed to be a half sine function with 10 N-power and 0.01 s-duration. The y-directional acceleration responses are measured at nine points (i.e., 1-9) on the top of the caisson caps as shown in Fig. 3.3. The sampling frequency is set as 1 kHz.

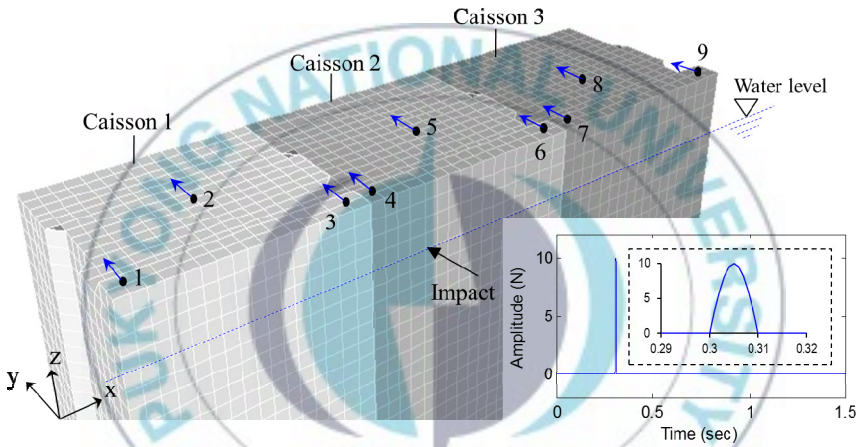

Fig. 3.3 Impact excitation and acceleration acquisition points

Fig. 3.4 shows acceleration signals in y-direction of points 2, 5 and 8. It is observed that the vibration of Caisson 2 is propagated into Caisson 1 and Caisson 3. However, the vibration amplitude of the unexcited caisson are only about a half of that of the excited one. This implies that a certain amount of energy is apparently subtracted from the excited caisson by wave propagation along the caisson system. This observation is similar to previous experimental studies reported by Lamberti and Martinelli (1998).

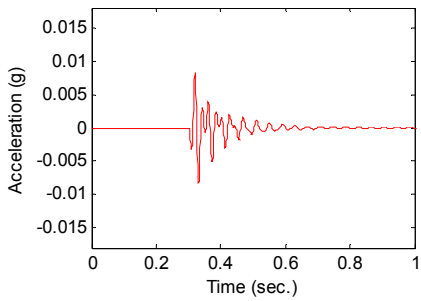

(a) Point 2 (Caisson 1)

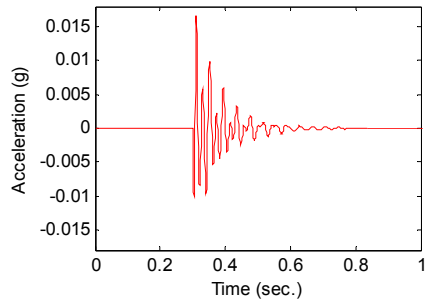

(b) Point 5 (Caisson 2)

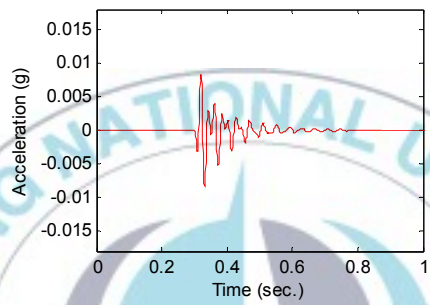

(c) Point 8 (Caisson 3)

Fig. 3.4 Y-directional acceleration signals of 3-D FE model

3.3.3 Vibration Modal Analysis

FDD Method

The frequency domain decomposition (FDD) method (Otte et al., 1990; Yi and Yun, 2004) is used to extract modal parameters such as natural frequency and mode shape. The singular values of the power spectral density (PSD) function matrix $S(\omega)$ are used to estimate the natural frequencies instead of the PSD functions themselves as follows:

$$S(\omega) = U(\omega)^T \Sigma(\omega) V(\omega) \tag{3.2}$$

where Σ is the diagonal matrix consisting of the singular values $(\sigma_i's)$ and U and V are unitary matrices. Since $S(\omega)$ is symmetric, U becomes equal to V. In this FDD method, the natural frequencies can be determined from the peak frequencies of the singular value, and the mode shape from any of the column vectors of $U(\omega)$ at the corresponding peak frequencies. Generally

the first singular value $\sigma_1(\omega)$ among σ_i's $(i=1, \ldots, N)$ is used to estimate the modal parameters except in some special cases such as with two or more identical excitations.

Modal Parameters

The y-directional acceleration responses measured at points 1, 3, 4, 6, 7 and 9 on the top of the caissons (see Fig. 3.3) are used to extract natural frequencies and mode shapes of the 3-D FE model. The singular values of the FDD procedure are shown in Fig. 3.5. In the frequency range of 0-200 Hz, three peaks that are selected for the target modes are 25.33 Hz, 47.59 Hz and 71.32 Hz, as listed in Table 3.3. The corresponding mode shapes are shown in Fig. 3.6. It is noted in the figure that the three caissons mostly move together in the same phase for mode 1 and mode 3 while the opposite phase is observed for the mode 2.

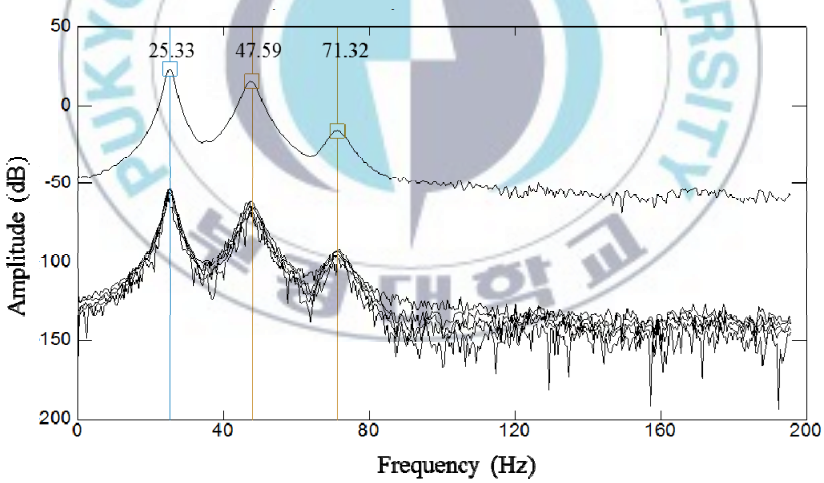

Fig. 3.5 Singular values of FDD procedure for 3-D FE model

Table 3.3. Natural frequencies of 3-D FE model

Natural frequency (Hz)		
Mode 1	Mode 2	Mode 3
25.33	47.59	71.32

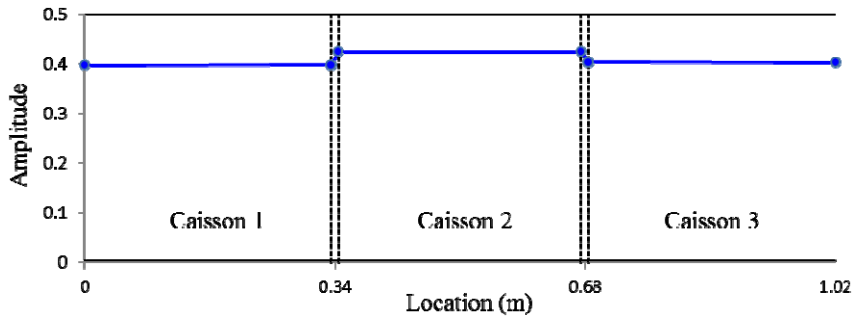

(a) Mode 1

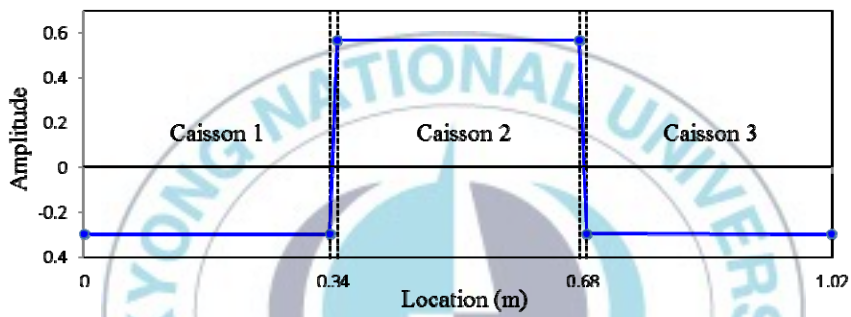

(b) Mode 2

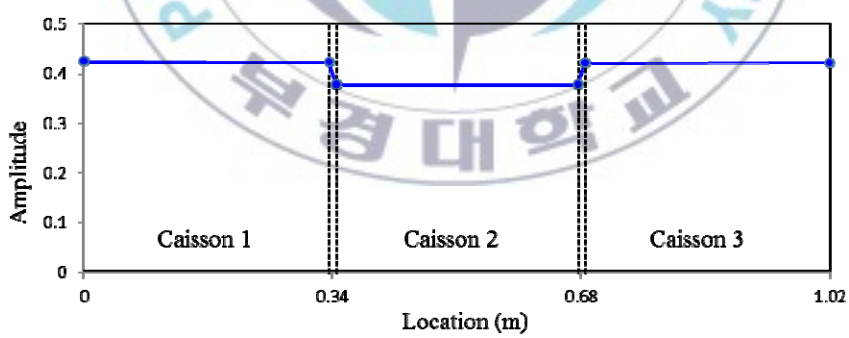

(c) Mode 3

Fig. 3.6 Y-directional mode shapes of 3-D FE model

3.4 Simplified Model of 3-D FE Simulation

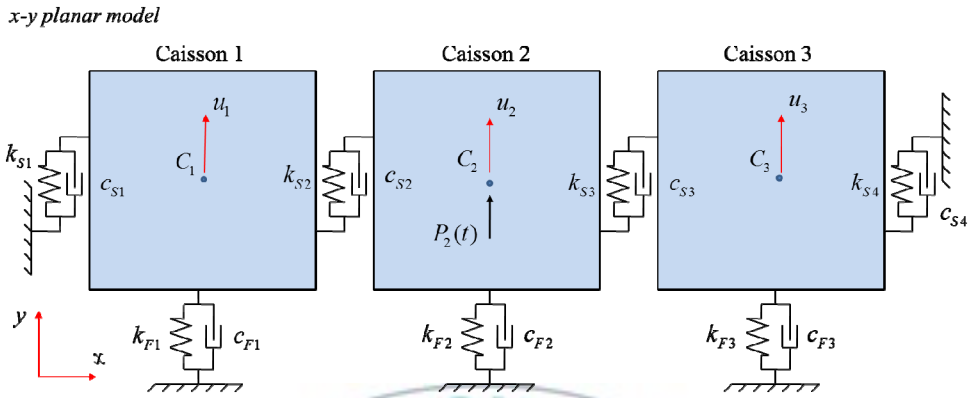

Fig. 3.7 Simplified model of 3-D FE simulation

The simplified model of the 3-D FE model is established using the proposed theoretical model (in Chapter 2), as shown in Fig. 3.7. An impact force $P_2(t)$ in y-direction is placed at Caisson 2 to excite the caisson system. The function of impact excitation $P_2(t)$ is described in Fig. 3.3. Structural parameters of the simplified model are determined as follows:

Mass Matrix

By using Eqs. (2.7)-(2.9), the mass parameters of the simplified model of the 3-D FE model are computed as:

$$m_1 = m_2 = m_3 = 100.43 + 42.68 + 6.40 = 149.52 \; kg \tag{3.3}$$

Then, from Eq. (2.3), the mass matrix is obtained as:

$$[M] = \begin{bmatrix} 149.52 & 0 & 0 \\ 0 & 149.52 & 0 \\ 0 & 0 & 149.52 \end{bmatrix} kg \tag{3.4}$$

Stiffness Matrix

The stiffness parameters are determined by matching vibration responses of the simplified model and the 3-D FE model using try-and-error method. The modulus of subgrade reaction of the foundation mound is selected as $25x10^6$ N/m^3 which is equivalent with that of medium dense sand (Bowles, 1996). By using Eq. (2.10), the spring constants of the foundation mound are calculated as:

$$k_{F1} = k_{F2} = k_{F3} = 25x10^6 x0.34x0.34 = 2.89x10^6 N/m \tag{3.5}$$

By assuming $k_{S1} = k_{S4} = 0.5k_{S2} = 0.5k_{S3}$ (Martinelli and Lamberti, 2011), the stiffness of the middle and last shear-keys are obtained as:

$$k_{S2} = k_{S3} = 1.1x2.89x10^6 = 3.179x10^6 N/m \tag{3.6a}$$

$$k_{S1} = k_{S4} = 0.5k_{S2} = 0.5k_{S3} = 0.5x3.179x10^6 = 1.590x10^6 N/m \tag{3.6b}$$

On substituting Eqs. (3.8), (3.9) and (3.10) into Eq. (2.5), the stiffness matrix is obtained as:

$$[K] = 10^6 x \begin{bmatrix} 7.658 & -3.179 & 0 \\ -3.179 & 9.248 & -3.179 \\ 0 & -3.179 & 7.658 \end{bmatrix} N/m \tag{3.7}$$

Damping Matrix

For calculating the damping parameter, the first two natural frequencies (f_1 = 25.33 Hz and f_2 = 47.59 Hz) and the critical damping ratio (5%) of the 3-D FE model are utilized to calculate the two Rayleigh damping coefficients (see Eq. (2.15)). The calculated mass-proportional damping coefficients (α) and stiffness-proportional damping coefficient (β) are, respectively, 10.387 and 0.000218. Then, the damping matrix is computed using Eq. (2.12) as the following:

$$[C] = 10^3 x \begin{bmatrix} 3.223 & -0.693 & 0 \\ -0.693 & 3.569 & -0.693 \\ 0 & -0.693 & 3.223 \end{bmatrix} Ns/m \tag{3.8}$$

Equations of Motion

Substituting Eq. (3.4), (3.7) and (3.8) into Eq. (2.2a), the equations of motion of the target caisson breakwater are written as:

$$\begin{bmatrix} 149.52 & 0 & 0 \\ 0 & 149.52 & 0 \\ 0 & 0 & 149.52 \end{bmatrix} \begin{Bmatrix} \ddot{u}_1 \\ \ddot{u}_2 \\ \ddot{u}_3 \end{Bmatrix} + 10^3 x \begin{bmatrix} 3.223 & -0.693 & 0 \\ -0.693 & 3.569 & -0.693 \\ 0 & -0.693 & 3.223 \end{bmatrix} \begin{Bmatrix} \dot{u}_1 \\ \dot{u}_2 \\ \dot{u}_3 \end{Bmatrix} + 10^6 x \begin{bmatrix} 7.658 & -3.179 & 0 \\ -3.179 & 9.248 & -3.179 \\ 0 & -3.179 & 7.658 \end{bmatrix} \begin{Bmatrix} u_1 \\ u_2 \\ u_3 \end{Bmatrix} = \begin{Bmatrix} 0 \\ P_2(t) \\ 0 \end{Bmatrix} \tag{3.9}$$

To solve the above equations of motion, the Runge–Kutta scheme supported in Matlab R2012b is utilized (Press et al., 1988). In the calculation process of vibration responses, the time interval is selected as 0.001 second.

3.5 Validation of Simplified Model's Vibration Responses

3.5.1 Vibration Response in Time Domain

Difference in Acceleration Acquisition Coordinates

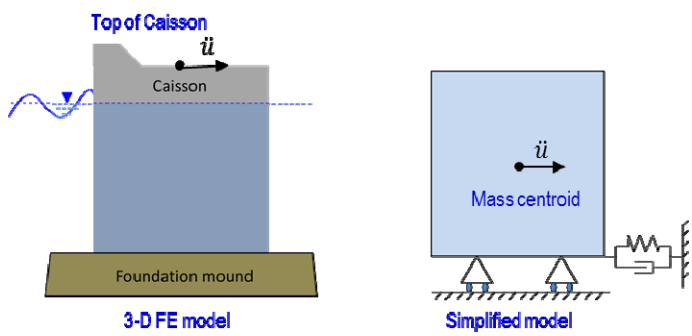

Fig. 3.8 Difference in acceleration acquisition coordinates between 3-D FE model and simplified model

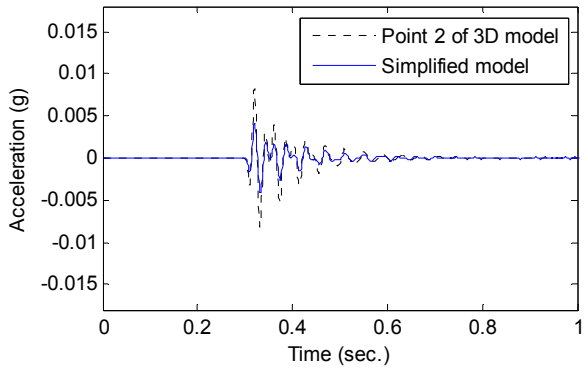

(a) Caisson 1

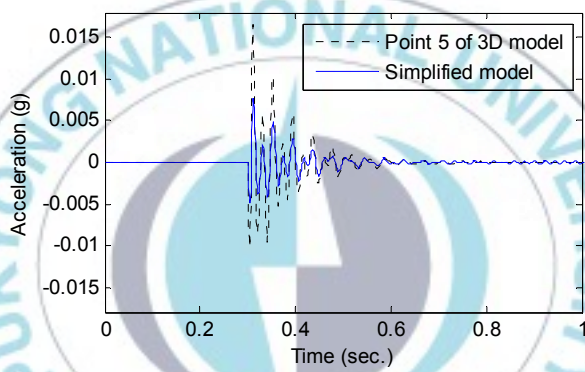

(b) Caisson 2

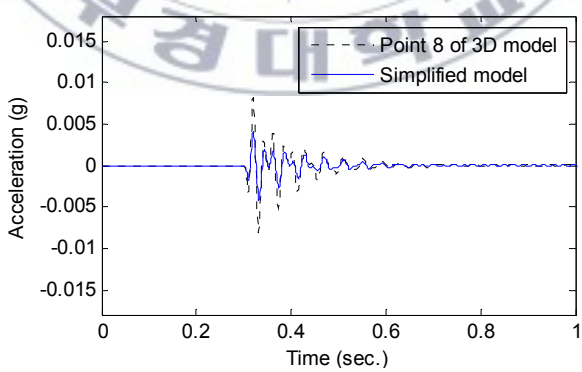

(c) Caisson 3

Fig. 3.9 Y-directional acceleration signals of 3-D FE model and simplified model with different acceleration acquisition coordinates

It is noted that the acceleration acquisition coordinate used in the simplified model is differed from that in the 3-D FE model, as described in Fig. 3.8. In the 3-D FE model, acceleration signals on the top of caissons are measured, whereas acceleration signals of the simplified model are computed at the mass centroids of the caissons. The difference in acceleration acquisition coordinates causes the difference in amplitudes of acceleration signals obtained from the simplified model and the 3-D FE model, as shown in Fig. 3.9. The vibration amplitudes of the simplified model are only about half of those of the 3-D FE model. To validate the accuracy of the simplified model in vibration analysis, the acceleration signals of the simplified model should be compared with those measured at the caissons' centroids of the 3-D FE model. However, it is almost impossible to measure directly these signals from real caisson breakwaters.

Estimation of Equivalent Vibration Responses

In order to match the acceleration acquisition coordinates between the simplified model and the 3-D FE model, the following procedure is performed by estimating the acceleration signals of the mass centroids of the caissons from the ones measured on the caisson caps in the 3-D FE model. Firstly, y-directional acceleration signals of additional locations on the front walls (i.e., points 10, 11 and 12) are measured as shown in Fig. 3.10a. By comparing the acceleration signals of the upper points (i.e., 3, 6 and 9) and the lower points (i.e., 10, 11 and 12), the inclinations of the caissons can be obtained. Secondly, the mass centroid of each caisson is computed considering the added mass of sea water by Eq. (3.1) and added mass of soil by Eq. (2.9), as indicated in Fig. 3.10b. Thirdly, for each caisson unit, the acceleration signal of the mass centroid (i.e., C_1, C_2 or C_3) is linearly-estimated based on its inclination (i.e., α_1, α_2 or α_3) and the measured signal at the top center location (i.e., point 2, point 5 or point 8).

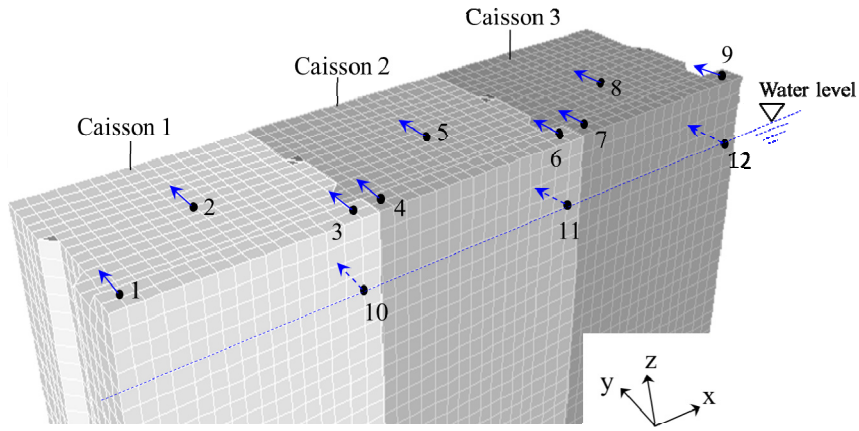

(a) Additional acceleration acquisition points 10, 11 and 12

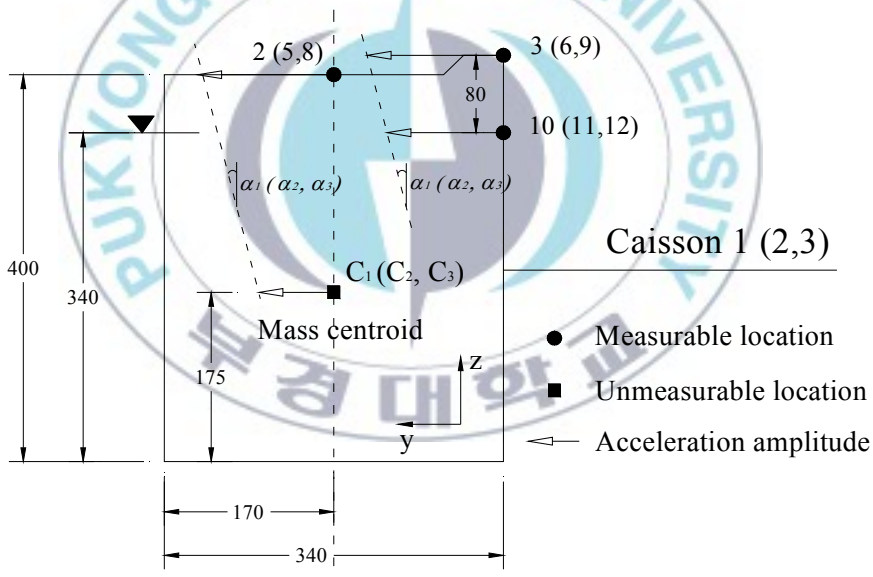

(

b) Linear relationships of acceleration signals

Fig. 3.10 Estimation of y-directional acceleration signals of caissons' centroids

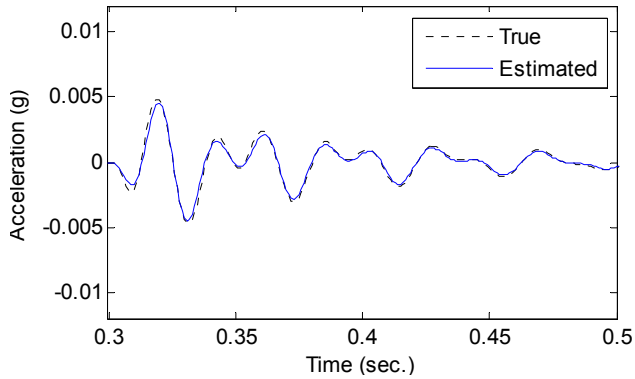

(a) Centroid of Caisson 1

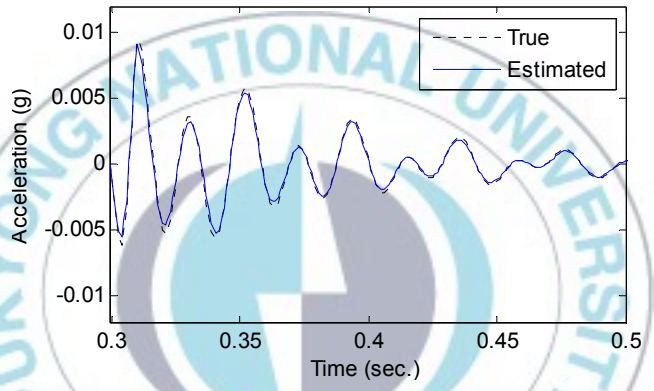

(b) Centroid of Caisson 2

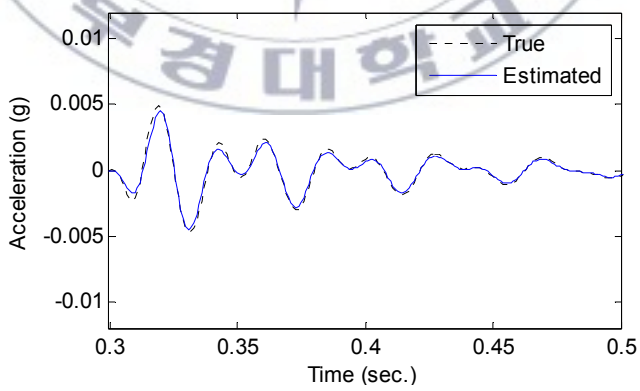

(c) Centroid of Caisson 3

Fig. 3.11 Y-directional acceleration signals of caissons' centroids in 3-D FE model

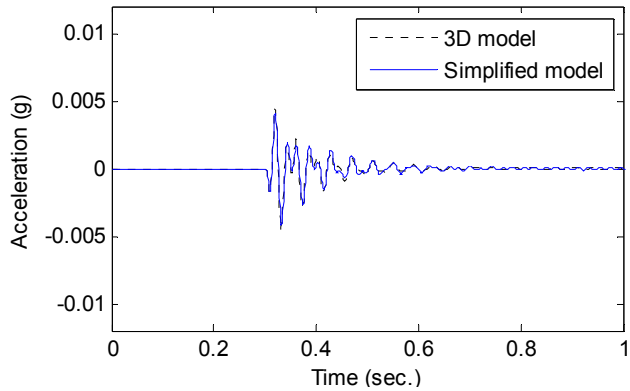

(a) Centroid of Caisson 1

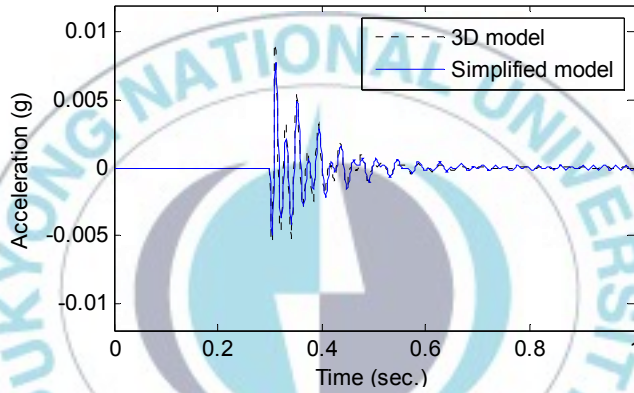

(b) Centroid of Caisson 2

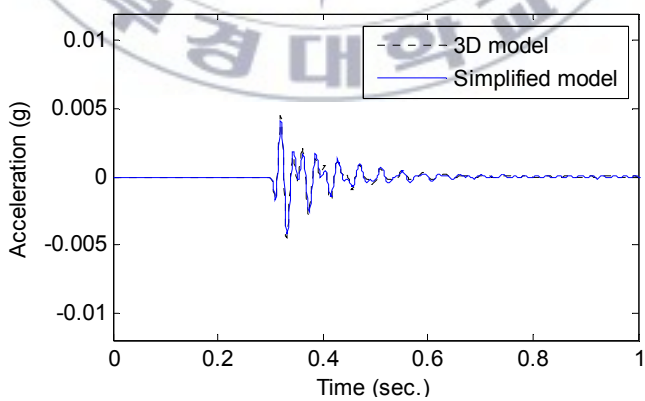

(a) Centroid of Caisson 3

Fig. 3.12 Y-directional acceleration signals of 3-D FE model and simplified model with equivalent acceleration acquisition coordinates

Fig. 3.11 shows the comparison between the estimated y-directional acceleration signals and the true ones of the caissons' centroids. It is noted that the true signals are measured directly at the caissons' centroids in the 3-D FE model. As observed in the figure, the estimated signals show good agreement with the true ones. Next, the estimated y-directional acceleration signals at the caissons' centroids in the 3-D FE model are used to compare with those of the simplified model, as sketched in Fig. 3.12. It can be seen in the figure that the signals of both models are well-matched.

3.5.2 Vibration Response in Frequency Domain

The PSDs of y-directional acceleration signals of the caissons' centroids are computed using Fast Fourier Transform (FFT) for the both models (i.e., simplified model and 3-D FE model), as shown in Fig. 3.13. It can be seen that the magnitudes and frequencies of the first two peaks obtained from the two models are well-matched. The FDD method (Otte et al., 1990; Yi and Yun, 2004) is performed to extract modal parameters from the acceleration signals. The extracted mode shapes and corresponding natural frequencies are sketched in Fig 3.14 and given in Table 3.4, respectively. It can be seen that the modal parameters of the simplified model are similar to those of the 3-D FE model.

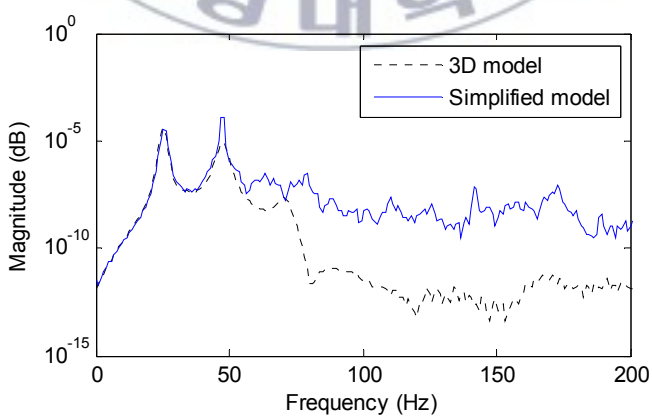

(a) Centroid of Caisson 1

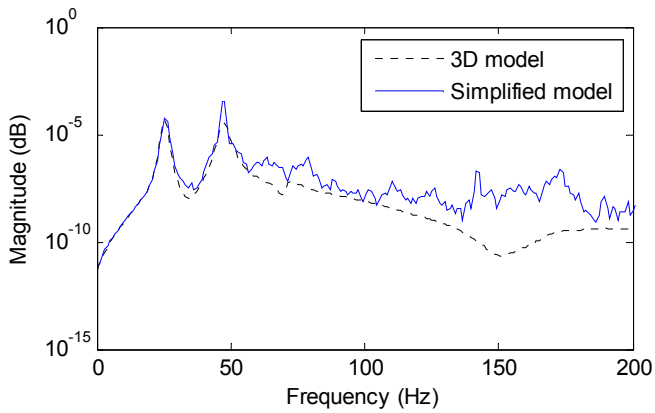

(b) Centroid of Caisson 2

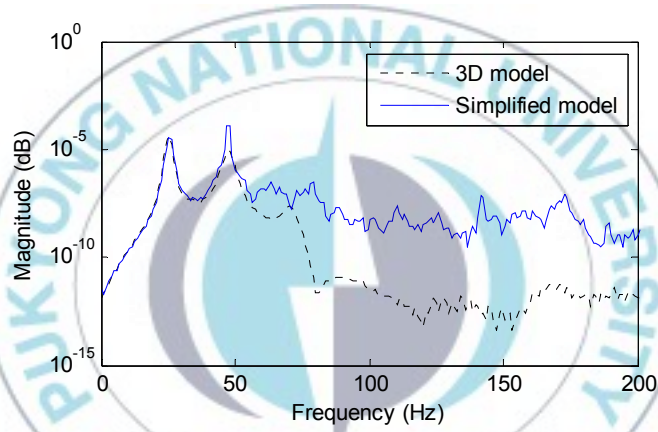

(b) Centroid of Caisson 3

Fig. 3.13 The PSDs of y-directional acceleration signals 3-D FE model and simplified model

Table 3.4 Natural frequencies of 3-D FE model and simplified model

Mode	Natural frequency of target caisson breakwater (Hz)		
	FE model	Simplified model	Variation
Mode 1	25.33	25.88	2.13%
Mode 2	47.59	47.36	-0.49%

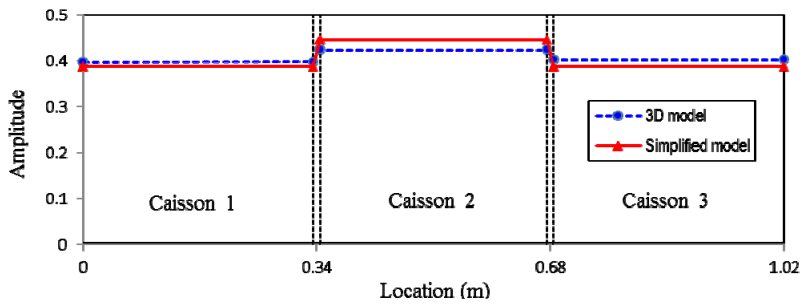

(a) Mode 1

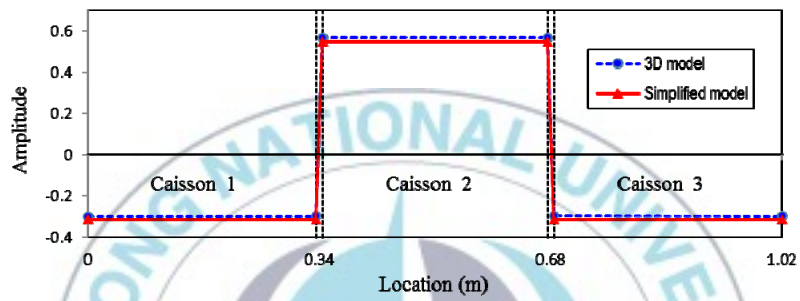

(b) Mode 2

Fig. 3.14 Y-directional mode shapes of 3-D FE model and simplified model

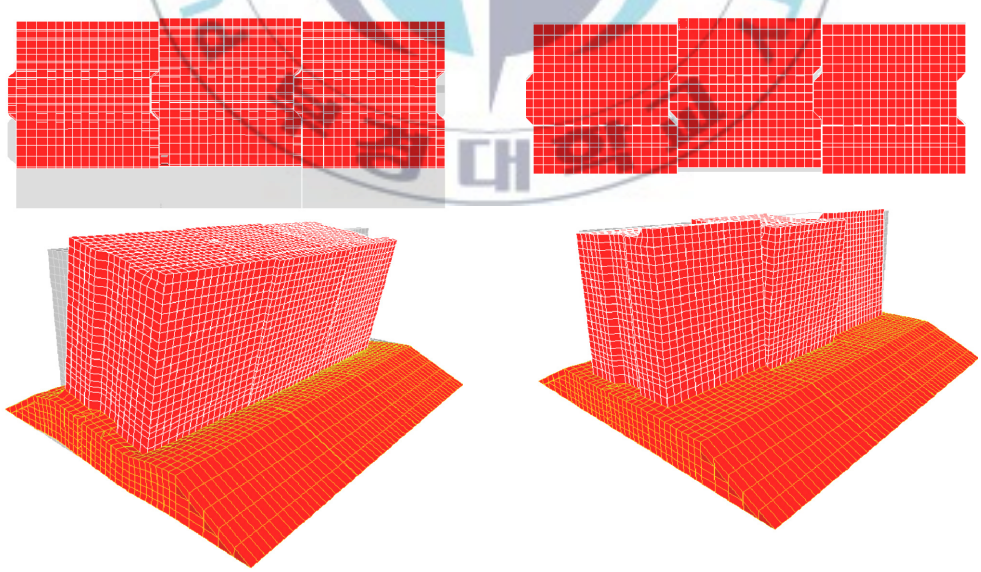

(a) Mode 1 (b) Mode 2

Fig. 3.15 Mode shapes of 3-D FE model by modal analysis

In order to improve the understanding of mode shapes of target caisson structure, modal analysis of the 3-D FE model is carried out in SAP2000 software. The first and second mode shapes of the target caisson breakwater are shown in Fig. 3.15. It is observed that three caissons mostly move together in the same phase for the first mode, but in the opposite phase for the second mode. These results are well comparable with those sketched in Fig. 3.14.

From these above observations, it is concluded that the simplified model of the interlocked caissons successfully represents the horizontal vibrations of the 3-D FE model. Hence, the proposed model can be used for dynamic analysis of interlocked caisson systems.

CHAPTER 4
FEASIBILITY OF SIMPLIFIED MODEL FOR STRUCTURAL DAMAGE ASSESSMENT

4.1 Introduction

In this chapter, the simplified model of the interlocked caissons is employed for the structural damage assessment. Firstly, a damage detection method is formulated on the basic modal strain energy (MSE)-based damage detection theories. Secondly, several damage cases are simulated in the structure-foundation interface of the 3-D FE model with regarding the loss of foundation materials. Thirdly, the MSE-based method is performed to predict damaged caissons in the 3-D FE model.

4.2 Modal Strain Energy-based Damage Detection

The simplified model of the interlocked caissons is utilized to design a damage detection model on the basic MSE-based damage detection method by Kim et al. (2002). For a linear, undamaged caisson system, as shown in Fig. 2.2, the i^{th} modal strain energy, U_i, is written by:

$$U_i = \frac{1}{2}\sum_{j=1}^{nc} \phi_{ij}^2 k_{F_j} + \frac{1}{2}\sum_{j=1}^{n} (\phi_{ij} - \phi_{ij-1})^2 k_{S_j} \tag{4.1}$$

where nc is the number of caisson units; n is the number of shear-key connections; ϕ_{ij} is the i^{th} modal displacement at the j^{th} caisson; k_{Fj} represents the stiffness of the j^{th} caisson's foundation; and k_{Sj} is the stiffness of the j^{th} shear-key connection.

The contribution of the j^{th} caisson's foundation to the i^{th} modal strain energy, U_{ij}, is defined as:

$$U_{ij} = \frac{1}{2}\phi_{ij}^2 k_{F_j} \tag{4.2}$$

Then, the fraction of the undamaged modal strain energy (i.e., the undamaged modal sensitivity) of the i^{th} mode and the j^{th} caisson is given by:

$$F_{ij} = \frac{U_{ij}}{U_i} \tag{4.3}$$

For the caisson system with only foundation damage, the damaged modal sensitivity of the i^{th} mode and the j^{th} caisson can be expressed as:

$$F_{ij}^{*} = \frac{U_{ij}^{*}}{U_i^{*}} \tag{4.4}$$

in which the quantities U_{ij}^{*} and U_i^{*} are calculated by:

$$U_{ij}^{*} = \frac{1}{2}\phi_{ij}^{*2} k_{F_j}^{*} \tag{4.5}$$

$$U_i^{*} = \frac{1}{2}\sum_{j=1}^{nc} \phi_{ij}^{*2} k_{F_j}^{*} + \frac{1}{2}\sum_{j=1}^{n} (\phi_{ij}^{*} - \phi_{ij-1}^{*})^2 k_{S_j} \tag{4.6}$$

For damage localization in the caisson system, a damage index η_j for the j^{th} caisson is defined via the ratio between the relative change in the modal sensitivity for the i^{th} mode with respect to the j^{th} caisson and the relative change in the stiffness of the j^{th} caisson's foundation as follows:

$$\eta_j = \frac{F_{ij}^{*} / F_{ij}}{k_{F_j}^{*} / k_{F_j}} \tag{4.7}$$

in which $\eta_j > 1$ indicates damage at the j^{th} caisson.

On substituting Eqs. (4.2), (4.3), (4.4) and (4.5) into Eq. (4.7), and by rearranging, the damage localization index η_j of the j^{th} caisson is simplified as the following:

$$\eta_j = \frac{\phi_{ij}^{*2} U_i}{\phi_{ij}^{2} U_i^{*}} \tag{4.8}$$

in which the i^{th} modal strain energies of pre- and post-damage cases can be expressed as:

$$U_i = \frac{1}{2}\lambda_i M_i \tag{4.9a}$$

$$U_i^* = \frac{1}{2}\lambda_i^* M_i^* \tag{4.9b}$$

where M_i and M_i^* are the i^{th} modal masses; λ_i and λ_i^* are the i^{th} eigenvalues. It is assumed that the i^{th} modal mass remains unchanged during the damaging event. Then, the relationship between the quantities U_i and U_i^* is simplified as:

$$\frac{U_i}{U_i^*} = \frac{\lambda_i}{\lambda_i^*} \tag{4.10}$$

By substituting Eq. (4.10) into Eq. (4.8), a damage localization index η_j of the j^{th} caisson is computed for nm measured modes as follows:

$$\eta_j = \frac{\sum_{i=1}^{nm} \phi_{ij}^{2*} \lambda_i}{\sum_{i=1}^{nm} \phi_{ij}^2 \lambda_i^*} \tag{4.11}$$

in which the components of the right hand side of Eq. (4.11) are measurable from the real caisson structure.

If we treat damage location indices as normally distributed random variables, the normalized damage indices are defined according to the standard rule as:

$$Z_j = \frac{(\eta_j - \mu_\eta)}{\sigma_\eta} \tag{4.12}$$

where μ_η and σ_η are the mean and the standard deviation of the collection of η_j values, respectively. Next, the damage is localized utilizing hypothesis testing. The null hypothesis (i.e., H_o) is that the structure is undamaged at the j^{th} element and alternate hypothesis (i.e., H_1) is that the structure is damaged at the j^{th} element. For damage localization, the following decision

rule is defined: first, select H_1 if $Z_j < Z_o$; or choose H_o if $Z_j > Z_o$, where Z_o is statistical confidence level of the localization test.

4.3 Verification of MSE-based Damage Detection

4.3.1 Description of Simulated Damage

As a damage scenario, it is assumed that the structure-foundation interface of the caissons is scoured under extreme wave loading. Three damage cases of the foundation (i.e., Damage 1, Damage 2 and Damage 3) are simulated by removing armor gravel elements as shown in Fig. 4.1. Only single damage is made in each damage scenario. The percentage loss of the gravel layer of Caisson 1 in Damage 1, of Caisson 2 in Damage 2 and of Caisson 3 in Damage 3 are 2.7%, 10.5% and 6.9%, respectively. In Damage 2 and Damage 3, the damaged areas are expanded to the foundation-caisson contact region.

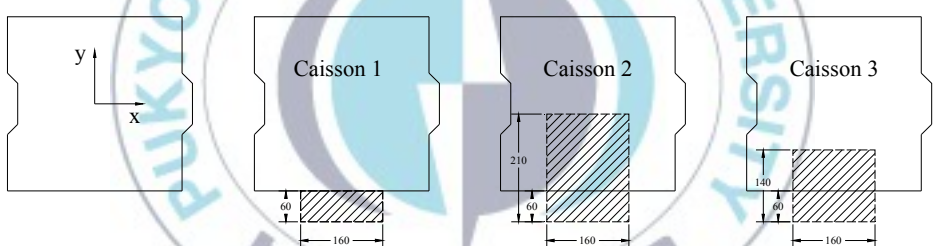

(a) Undamaged (b) Damage 1 (c) Damage 2 (d) Damage 3

Fig. 4.1 Foundation damage cases

4.3.2 Damage Monitoring Results

For detecting foundation damage, y-directional acceleration signals of the points 2, 5 and 8 of the 3-D FE model (see Fig. 3.3) before and after the damaging event are measured. Next, the natural frequencies and mode shapes are extracted from those signals (by FDD method). Table 4.1 summarizes the natural frequencies of the caisson system for all damage cases. Only the first and the second modes are listed due to that these modes well match with those of the simplified model. As given in the table, natural frequencies are decreased according to the damage growth. Fig. 4.2 shows

the y-directional mode shapes of the 3-D FE model. It is observed that the relative motions between caissons are changed after the damaging events, and the first mode is more sensitive to the foundation damage than the second one.

Table 4.1. Natural frequencies of 3-D FE model with foundation damage

Case	Damage scenario	Natural frequency (Hz)	
		Mode 1	Mode 2
Undamaged	-	25.33	47.59
Damage 1	Removed 2.7% of armor gravel	25.13 (-0.78%)	47.54 (-0.11%)
Damage 2	Removed 10.5% of armor gravel	24.77 (-2.25%)	46.98 (-1.31%)
Damage 3	Removed 6.9% of armor gravel	24.85 (-1.92%)	47.43 (-0.33%)

Parentheses indicate variation (%) of natural frequencies with respect to undamaged case

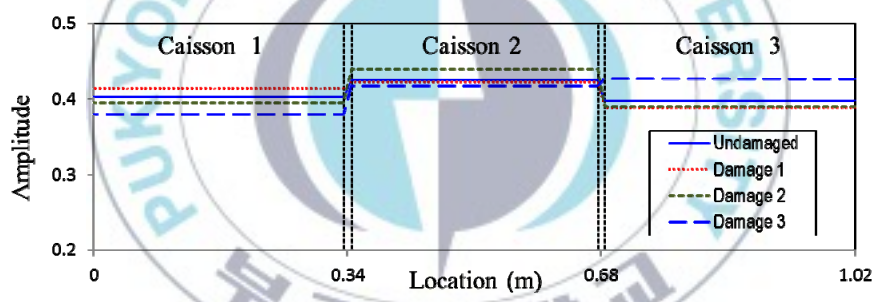

(a) Model 1

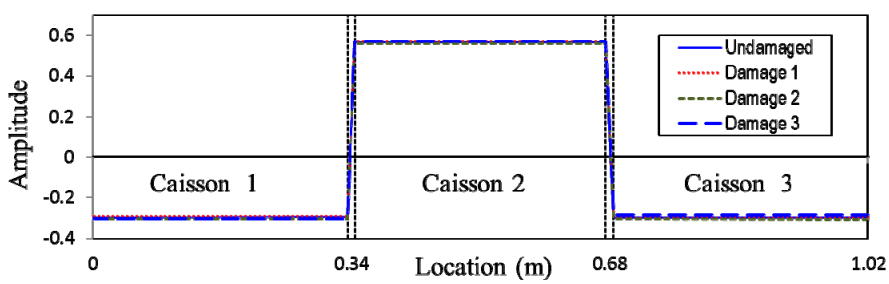

(b) Mode 2

Fig. 4.2 Y-directional mode shapes of 3-D FE model with foundation damage

Next, the MSE-based method is employed to predict damage locations in the 3-D FE model. The normalized damage index is calculated by Eqs. (4.11) and (4.12). Damage localization results are illustrated in Fig. 4.3. Here, the criterion value Z_o is chosen as 1.26 which is corresponding to the confidence level of 90%. It is found that for all damage cases with different damage severities, the MSE-based method has successfully localized the damaged caissons.

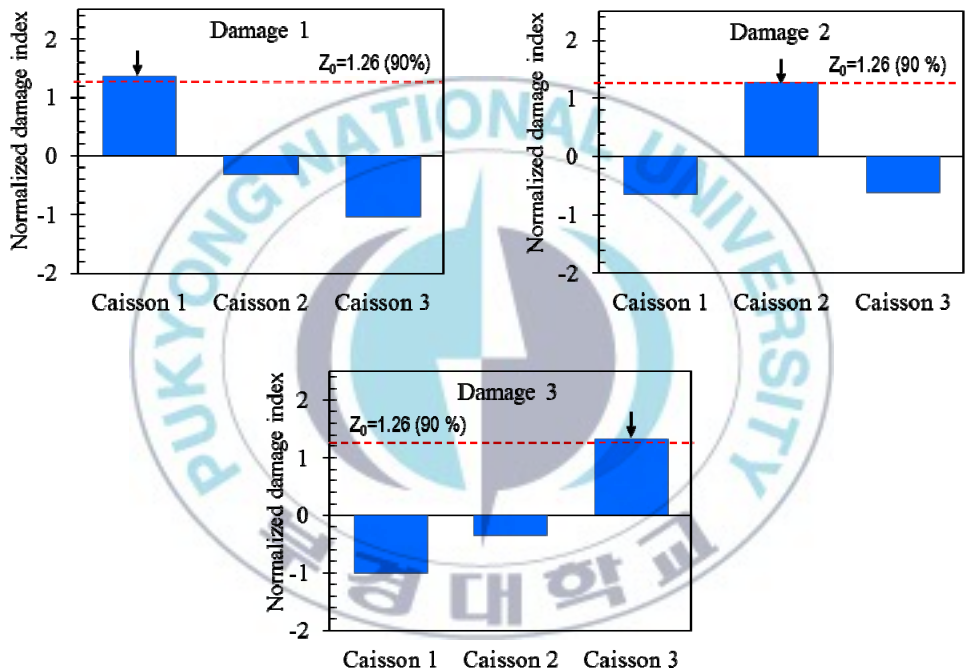

Fig 4.3 Damage localization results in 3-D FE model

CHAPTER 5
CONCLUSION

In this study, a simplified model of interlocked caisson system, which can be used for dynamic analysis and damage assessment, was presented. The following approaches are performed to obtain the objective. Firstly, a conceptual dynamic model of the interlocked caisson system was designed on the basis of the characteristics of existing harbor caisson structures. A mass-spring-dashpot model considering only the sway motion was proposed. In the simplified model, each caisson unit was connected to adjacent ones by adding springs and dashpots to represent the condition of the interlocking mechanism. Secondly, the simplified model of the interlocked caisson system was evaluated for vibration analysis. A 3-D finite element model of the caisson system was utilized to examine the accuracy of the simplified model's vibration responses. Thirdly, the simplified model of the caisson system was employed for damage assessment. A damage detection method based on modal strain energy is formulated to localize damage in the caisson system.

From the observations in this study, the following conclusions have been made:

(1) The proposed planar model successfully estimated the horizontal vibration of the caisson system. The vibration features (i.e., power spectral density, natural frequency and mode shape) of the simplified model were well consistent with those of the 3-D FE model. Hence, the planar model was reliable for the dynamic analysis of the caisson system.

(2) The MSE-based damage detection method formulated for the simplified planar model successfully identified damage locations with high confidence level.

Despite the feasibility of the proposed planar model of the caisson system for vibration analysis and damage estimation, several issues still

remain. The damage severity in the foundation should be studied extensively by quantifying its magnitude. The proposed simplified model should be experimentally verified on real or lab-scaled caisson breakwaters for the structural health assessment.

REFERENCES

ACI Committee 318 (2005), "Building Code Requirement for Structural Concrete (ACI 318-05) and Commentary (318R-05)", *American Concrete Institute*, Farmington Hills, MI, USA.

Doebling. S.W., Farrar, C.R. and Prime, M.B. (1998), "A Summary Review of Vibration-based Damage Identification Method", *The Shock and Vibration*, Digest, Vol. 30(2), 91-105.

Franco, L. (1994), "Vertical Breakwaters: the Italian Experience", *Coastal Engineering*, Vol. 22, 3-29.

Gao, M., Dai, G. Y., and Yang, J. H. (1988), "Dynamic Studies on Caisson-type Breakwaters", *Proc. 21st Conf. on Coastal Eng.*, Torremolinos, Spain, 2469-2478.

Glisic, B., Inaudi, D., Lau, J.M., Mok, Y.C., and Ng, C.T. (2005), "Long-Term Monitoring of High-Rise Buildings Using Long-Gage Fiber Optic Sensors", *7th Int. Conf. on Multi-Purpose High-Rise Towers and Tall Buildings*, Dubai, UAM.

Goda, Y. (1994), "Dynamic Response of Upright Breakwater to Impulsive Force of Breaking Waves", *Coastal Engineering*, Vol. 22, 135-158.

Ho, D.D., Lee, P.Y., Nguyen, K.D., Hong, D.S., Lee, S.Y., Kim, J.T., Shin, S.W., Yun, C.B. and Shinozuka, M. (2012), "Solar-powered Multi-scale Sensor Node on Imote2 Platform for Hybrid SHM in Cable-stayed Bridge", *Smart Structures and Systems*, Vol. 9(2), 145-164.

Jang, S.A., Jo, H., Cho, S., Mechitov, K.A., Rice, J.A., Sim, S.H., Jung, H.J., Yun, C.B., Spencer, Jr., B.F., and Agha, G. (2010), "Structural Health Monitoring of a Cable-stayed Bridge using Smart Sensor Technology: Deployment and Evaluation", *Smart Structures and Systems*, Vol. 6(5-6), 439-459.

Kim, D.K., Ryu, H.R., Seo, H.R. and Chang, S.K. (2005), "Earthquake Response Characteristics of Port Structure according to Exciting Frequency Components of Earthquakes", *J. Korean Soc. Coast.Ocean Eng.*, Vol. 17(1), 41-46.

Kim, J.T. and Stubbs, N. (1995), "Damage localization accuracy as a function of model uncertainty in the I-40 bridge over the Rio Grande", *Proc. of SPIE*, San Diego, USA.

Kim, J. T., and Stubbs, N. (2002), “Improved Damage Identification Method Based on Modal Information’, *Journal of Sound and Vibration*, Vol. 252(2), 223-238.

Kobayashi, M., Tersashi, M., and Takahashi, K. (1987), "Bearing Capacity of Rubble Mound Supporting a Gravity Structure", *Report of Port and Harbor Research Institute*, Vol. 26(5), 234-241.

Koo, K.Y., Lee, J.J., Yun, C.B. and Kim, J.T. (2009), “Damage Detection in Beam-like Structures using Deflections obtained by Modal Flexibility Matrices”, *Advances in Science and Technology*, 56, 483-488.

Lamberti, A., and Martinelli, L. (1998) “Prototype Measurements of the Dynamic Response of Caisson Breakwaters,” *Proc. 26th ICCE*, Copenhagen, Denmark.

Lee, S. Y., Lee, S. R., and Kim, J. T. (2011), "Vibration-based Structural Health Monitoring of Harbor Caisson Structure", *Proc. of SPIE*, USA.

Lee, S. Y., Nguyen, K. D., Huynh, T. C., Kim, J. T., Yi, J. H. and Han, S. H. (2012), "Vibration-Based Damage Monitoring of Harbor Caisson Structure with Damaged Foundation-Structure Interface", *Smart Structures and Systems*, Vol. 10(6), 517-547.

Look, B. (2007), "Handbook of Geotechnical Investigation and Design Tables", *Taylor & Francis.*

Maddrell, R. (2005), “Lessons Re-Learnt from the Failure of Marine Structures”, *Int. Conf. on Coastlines, Structures and Breakwaters, ICE*, 139-152.

Marinski, J.G., and Oumeraci, H. (1992), “Dynamic Response of Vertical Structures to Breaking Wave Forces – Review of the CIS Design Experience”, *Proc. 23rd Int. Conf. Coastal Eng.*, Venice, ASCE, New York, Vol. 2, 1357-1370.

Matlab R2012b, Inc. (2012), http://www.matlab.com

Otte, D., Van de Ponseele, P. and Leuridan, J. (1990), “Operational Shapes Estimation as a Function of Dynamic Loads”, *Proc. of IMAC*, Florida, USA.

Oumeraci, H. (1994), “Review and Analysis of Vertical Breakwater Failures – Lessons Learned”, *Coastal Engineering*, Vol. 22, 3-29.

Oumeraci, H., and Kortenhaus, A. (1994), “Analysis of the Dynamic Response of Caisson Breakwaters”, *Coastal Eng.*, Vol. 22, 159-183.

Oumeraci, H., Kortenhaus, H., Allsop, W., de Groot, M., Crouch, R., Vrijling, H., and Voortman, H. (2001), “Probabilistic Design Tools for Vertical Breakwaters”, *Swets & Zeitlinger B.V., Lisse*.

Pandey, A. K., and Biswas, M. (1994), “Damage Detection in Structures using Changes in Flexibility”, *Journal of Sound and Vibration*, Vol. 169(1), 3-17.

Park, J.H., Kim, J.T., Hong, D.S., Ho, D.D., Yi, J.H. (2009), “Sequential Damage Detection Approaches for Beams using Time-Modal Features and Artificial Neural Networks”, *Journal of Sound and Vibration*, Vol. 323(1), 451-474.

Park W. S., Lee, S. R., Lee, S. Y., and Kim, J. T., (2011), “Damage Monitoring in Foundation-Structure Interface of Harbor Caisson Using Vibration-based Autoregressive Model”, *Journal of Korean Society of Coastal and Ocean Engineers*, Vol. 23, No 1, pp. 18-25.

Press, W.H., Flannery, B. P., Teukolsky, S. A. and Vetterling, W. T. (1988), “Numerical Recipes – the Art of Scientific Computing”, *Cambridge University Press, Cambridge.*

Rechart, F. E., Hall Jr., J. R., Woods, R. D., (1970), “Vibration of Soils and Foundations”, *Prentice Hall Inc.*.

SAP2000, Inc. (2006), *http://www.sap2000.org*

Sekiguchi, H., and Ohmaki, S. (1992), "Overturning of Caisson by Storm Waves," *Soild and Found.*, Tokyo, Vol. 32(3), 144-155.

Sekiguchi, H., and Kobayashi, S. (1994), "Sliding of Caisson on Rubble Mound by Wave Force," *Proc. 13rd Int. Conf. on Soil Mech. And Found. Eng.,* Balkema, Rotterdam, The Netherlands, 1137-1140.

Smirnov, G.N., and Moroz, L.R. (1983), “Oscillations of Gravity Protective Structures of a Vertical Wall Type”, *IAHR, Proc. 20th Congress*, Vol. 7, 216-219.

Sohn, H., Farrar, C. R., Hemez, F. M., Shunk, D. D., Stinemates, D. W., Nadler, B. R. (2003), “A Review of Structural Health Monitoring Literature: 1996-2001”, *Los Alamos National Laboratory Report LA-13976-MS.*

Takahasi, S. (2002), “Design of Vertical Breakwaters”, *Port and Airport Research Institute*, Japan.

Tanimoto, K., and Takahashi, S. (1994), "Design and Construction of Caisson Breakwaters – the Japanese Experience", *Coastal Engineering*, Vol. 22, 3-29.

Taro, A., Masaharu, S., Ken-ichiro, S., Takashi, T., Daisuke, T., Geyong-Seon, Y., and Kenya, T. (2012), "Investigation of the Failure Mechanism of Kamaishi Breakwaters due to Tsunami – Initial Report Focusing on Hydraulic Characteristics", *Technical Note of The Port and Airport Research Institute*, No. 1251.

Vink, H.A.Th. (1997), "Wave Impacts on Vertical Breakwaters", *Master's thesis*, Faculty of Civil Engineering, Delft University of Technology, The Netherlands.

Westergaard, H.M. (1933), "Water Pressures on Dams during Earthquakes", *T. Am. Soc.*, Vol. 98(2), 418-432.

Wilson, E. L. (2004), Static and Dynamic Analysis of Structures (4th edition), *Berkeley, CA: Computers and Structures, Inc.*

Wong, K.Y. (2004), "Instrumentation and health monitoring of cable-supported bridges", *Structural Control Health Monitoring*, Vol. 11(2), 91-124.

Wu, X, Ghaboussi, J. and Garret, J.H., Jr. (1992), "Use of Neural Networks in Detection of Structural Damage", *Computers & Structures*, Vol. 42(4), 649-659.

Yamamoto, M., Endo, T., Hasegawa, A., and Tsunakawa, K. (1981), "Random Wave Tests on a Damaged Breakwater in Himekawa Harbor, Japan", *Coastal Engineering*, Vol. 5, 275-294.

Yang, Z., Elgamal, A., Abdoun, T. and Lee, C.J. (2001), "A Numerical Study of Lateral Spreading behind a Caissontype Quay Wall", *Proc. 4th Int. Conf. on Recent Adv. in Geot. Earthq. Eng. and Soil Dyn. and Symp.,* California, USA.

Yi, J.H., Park, W. S., Lee, S. Y., Kim, J. T., Seo, C. K. (2013), "Evaluation of Vibration Characteristics of Caisson-Type Breakwater Using Impact Vibration Tests and Validation of Numerical Analysis Model (in Korean)", *Journal of Korean Society of Coastal and Ocean Engineers,* Vol. 25, 1-10.

Yi, J.H., and Yun, C. B (2004), "Comparative Study on Modal Identification Methods using Output-Only Information", *Struct. Eng. Mech.,* Vol. 17(3-4), 445-456.

Yoon, H. S., Lee, S. Y., Kim, J. T., and Yi, J. H. (2012), "Field Implementation of Wireless Vibration Sensing System for Monitoring of Harbor Caisson Breakwaters," *International Journal of Distributed Sensor Networks*, Vol. 2012, 1-9.

Yun, C.B. and Bahng, E.Y. (2000), “Substructural Identification using Neural Networks”, Computers & Structures, Vol. 77(1), 41-52.

ACKNOWLEDGEMENTS

Foremost, I would like to express my deepest gratefulness to my advisor, Prof. Jeong-Tae Kim, for his excellent guidance, caring, patience, and providing me with an excellent atmosphere for doing research at Smart Structures Engineering Laboratory (SSeL), Pukyong National University, Busan, Korea.

Beside my advisor, I would like to thank the rest of my thesis committee: Prof. Won-Bae Na and Prof. Yun-Tae Kim, for their encouragement, useful comments, and helpful suggestions beyond the scope of this study. I am also grateful for the valuable lectures from Professors of Ocean Engineering Department at Pukyong National University.

I'm thankful to Ms. So-Young Lee, for helping me to do many research reports by Korean, and to all undergraduate students of SSeL, for giving me the pleasant time in laboratory. Further thanks goes to my friends in Pukyong National University: Mr. Niroopan Pararajasingam, Mr. Iqbal-Ali Husni, Mr. Hoang-Phuoc Ho, and Ms. Payuda Theppichai, for all the fun we had in the last two years.

My greatest appreciation goes to my closest friend, Mr. Khac-Duy Nguyen, who was always a great support in all my struggles and frustrations in my new life and studies in Korea. Cheers to Nguyen for being a great reliable person to whom I could always talk about my problems and excitements. Thanks him for questioning me about my ideas, helping me think rationally and even for hearing my problems.

I would like to thank to the Brain Korean 21 program of Korean Government, for their financial support during my Master course here.

Last but not the least, I would like to express my gratitude to my parents, elder sisters, younger brother, and my love. They were always there cheering me up and stood by me through the good times and bad.